ECCOMAS Congress 2016
VII European Congress on Computational Methods in Applied Sciences and Engineering
M. Papadrakakis, V. Papadopoulos, G. Stefanou, V. Plevris (eds.)
Crete Island, Greece, 5–10 June 2016

EFFICIENT NUMERICAL SIMULATION OF INDUSTRIAL SHEET METAL BENDING PROCESSES

Ch. Zehetner[1], P. Reimer[1], F. Hammelmüller[1], H. Irschik[2] and W. Kunze[3]

[1] Linz Center of Mechatronics GmbH
Altenbergerstrasse 69, 4040 Linz, Austria
e-mail: {christian.zehetner, paula.reimer, franz.hammelmueller}@lcm.at

[2] Johannes Kepler University of Linz
Altenbergerstrasse 69, 4040 Linz, Austria
hans.irschik@jku.at

[3] Salvagnini Maschinenbau GmbH
Dr. Guido Salvagnini-Straße 1, 4482 Ennsdorf, Austria
wolfgang.kunze@salvagninigroup.com

Keywords: plasticity, sheet metal bending, shell theory

Abstract. *In industrial production processes focus is given to high precision, quality, resource efficiency and productivity. In order to achieve these goals, efficient numerical simulation models are required. In the following, we consider an industrial sheet metal bending process, in which the sheet is fixed on one side and formed by a moving tool. On the one hand, there is a very large number of process parameters. On the other hand, the production sites are complex and have to be modelled in detail. Parameter studies are very extensive and take a large numerical effort. Therefore high efficient simulation tools are necessary to handle this challenge. In this paper two strategies for increasing the efficiency of modelling are investigated. First, the main focus is set to an efficient Finite Element model for sheet bending. Two Finite Element formulations are compared based on 3D-continuum elements and continuum shell elements. Secondly, a proper normalized formulation (similarity solution) of the bending process is derived starting from a reduced-order model, which subsequently is successfully applied to the complex bending process. Utilizing the concept of similarity, the number of cases in parameter studies can be reduced significantly.*

1 INTRODUCTION

In industrial metal forming processes, high versatility is claimed with respect to material types, geometric dimensions and process parameters. In order to control and optimize the production process, powerful simulation models are required. Usually, metal forming simulation models are very complex and highly non-linear. Thus, parameter studies are accompanied by a large computational effort such that an efficient simulation environment is required.

In sheet bending processes we deal with thin structures, which can be efficiently modelled by plate elements. In section 2, appropriate formulations are investigated, based on the bending of a one-side clamped plate. Using the powerful code ABAQUS, the results for continuum shell elements and three dimensional solid elements are compared. The goal is to find suitable configurations (mesh, element type, etc.) and the range of applicability of the specific elements.

A second important aspect is that the number of cases in parameter studies can be reduced significantly by using the concept of similarity, cf. [1] and [2] for the theory of similarity. Several combinations of parameters behave in a similar way. It is the challenge to find the appropriate parameter combinations, i.e. a reduced set of non-dimensional parameters describing the physical process without loss of information. In [3] this has been demonstrated for the bending of a cantilever beam subject to inertial loads arising in a drop test. In section 3, the similarity concept is applied to the one-side clamped plate and it is demonstrated how the number of dimensional parameters can be reduced by appropriate non-dimensional ones. This is first investigated analytically in the framework of a geometrically linearized elasto-plastic theory. A similarity formulation is derived which is successfully applied to the real large-deformation bending process afterwards.

2 FINITE ELEMENT MODEL OF SHEET BENDING

In the following a thin sheet of metal with length L, width B and thickness H is clamped on the left side and subject to a distributed force f per unit width at the right side as shown in Fig. 1. The total bending force is $F = fB$.

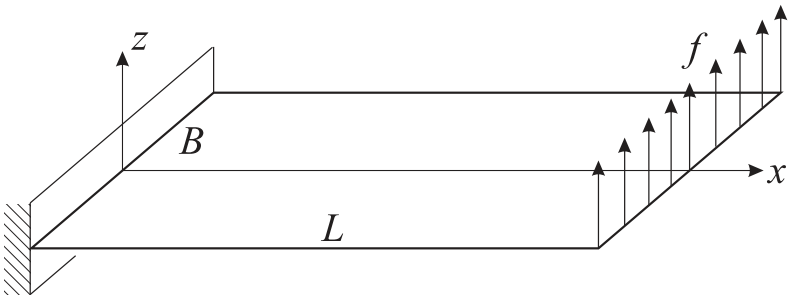

Figure 1: Bending of a plate

The material behavior is assumed to be elasto-plastic with exponential stress-strain relation of Ludwik's type, e.g. [3] and [4]. For a uni-axial state of stress the constitutive relations can be expressed as

$$\sigma = E\varepsilon \quad \text{for } \sigma \le \sigma_Y, \qquad \sigma = a\varepsilon^b \quad \text{for } \sigma \ge \sigma_Y, \tag{1}$$

where σ is the axial stress, ε the axial strain, E Young's modulus, a and b specify the exponential stress-strain relation, and σ_Y is the yield stress, following from solving Eq. (1) as

$$\sigma_Y = E\left(E/a\right)^{1/(b-1)}. \tag{2}$$

For this bending process, a Finite Element model has been implemented in ABAQUS, see [5] considering large strains. A quasi-static solution is computed with the implicit solver (ABAQUS standard).

2.1 Finite Element Discretization and Element Types

Figure 2 shows two discretizations of the plate. For numerical reasons, the clamping is here approximated by two elastic bodies which are fixed on the outer surfaces. The distributed force is applied by a moving elastic cylindrical body. Between the bodies contact is defined. Figure 2a shows a fine mesh with three-dimensional solid elements (C3D8R). On the other hand, the plate is discretized by continuum shell elements (SC8R) as defined in the ABAQUS documentation [5]. The continuum shell elements consider transverse shear stiffness as well as thickness contraction. They are capable for multi-layered shells. In the present context, two equal layers are used, where the continuum shell nodes work as super-elements, see Figure 2.

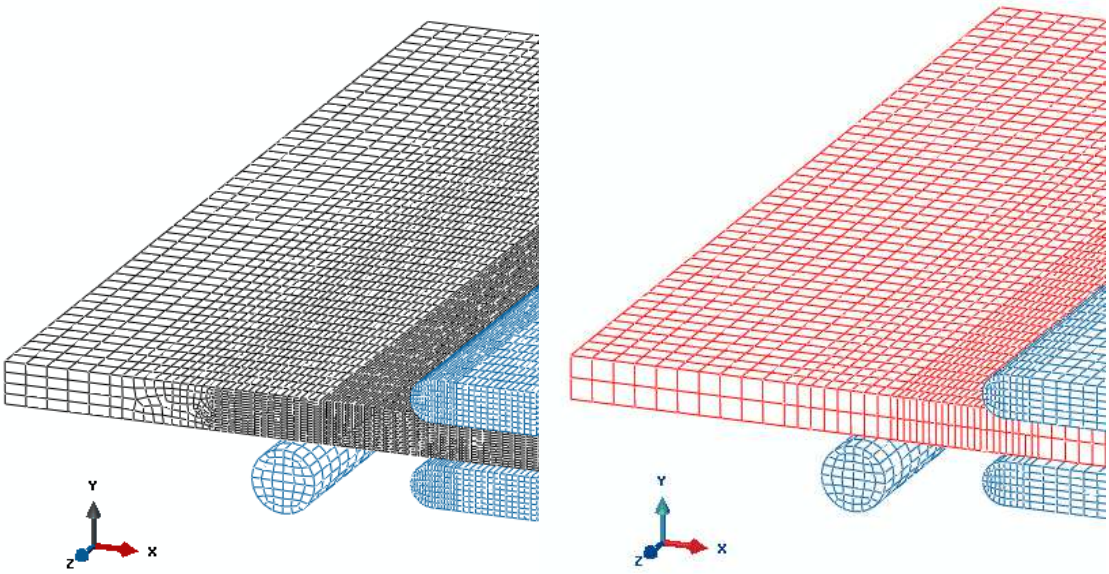

Figure 2: Finite Element models (a) 3D-continuum elements, (b) continuum shell elements

2.2 Results

Figure 3 shows a comparison of the deformed configuration of the two element types for a bending angle of about 90°. Near the clamping there are slight differences in the displacement field since the cross-sectional warping is restricted in the continuum shells. Note that even for large bending angles the cross-sections remain approximately plane, such that it is possible to obtain suitable results by plate theory.

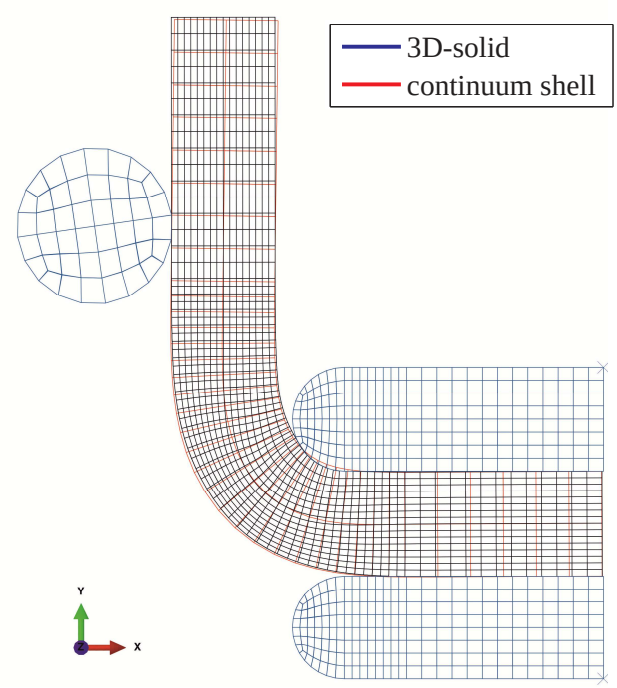

Figure 3: Deformed shape

Secondly, the contact force between cylinder and plate is compared, also denoted as bending force. The results are shown in Fig. 4, where a normalized resulting contact force is shown as a function of the bending angle. The results show a good correspondence for all bending angles.

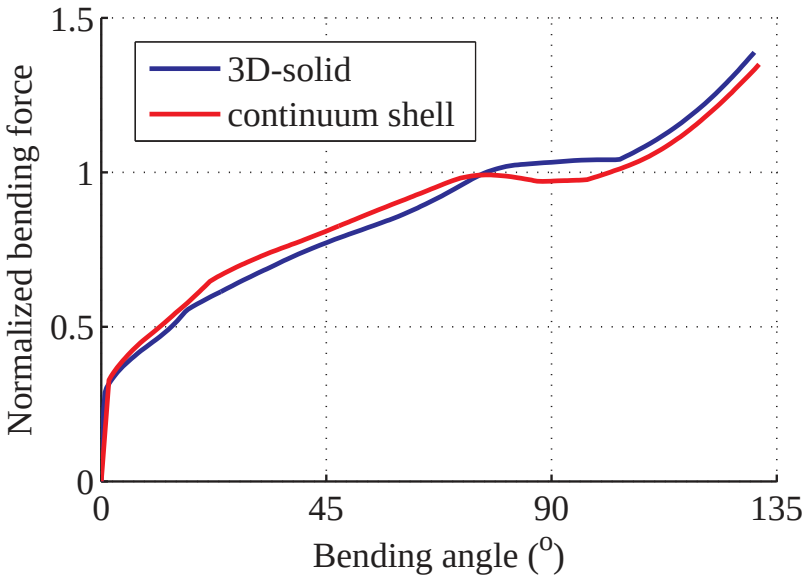

Figure 4: Comparison of the contact force

Finally the distribution of stress in the plate is compared for an angle of 90°. Figure 5 shows the result of a normalized v.Mises stress along the normalized coordinate *x/L* (see Fig. 1) on the top (a) and on the bottom (b) of the plate. The results for 3D-solids and continuum shells show a good coincidence especially for the maximum values. In this range the normal

strains are dominating, i.e. bending and longitudinal extension. In the surrounding of the clamping and near the contact with the cylinder, there are some differences resulting from a more general state of stress which is not represented in such detail by the continuum shell elements. Nevertheless, the result of the contact force is reliable as shown in Figure 4.

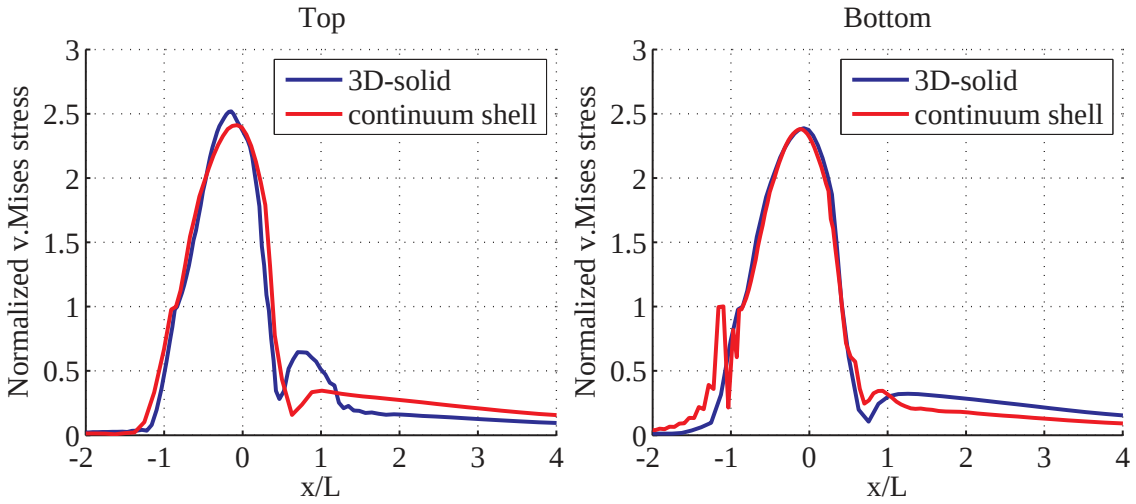

Figure 5: v.Mises stress

Finally the computation time is compared in Table 1 for the two element types. With the continuum shells, a speed-up factor of about 40 has been obtained.

Element type	Total CPU time (sec)
3D-solid	140356
Continuum shell	3672

Table 1: Computation time

2.3 Discussion

In sections 2.1-2.2 the results of plate bending obtained with 3D-solid and continuum shell elements have been compared. Displacement and stress fields as well as the resulting bending force show a good coincidence even for large deformations. The advantage of continuum shells is a significant reduction of computation time.

Since the bending process can be modelled with shell elements with satisfactory accuracy, it appears to be feasible to derive a non-dimensional (similarity) formulation of the complex bending process by using a strongly reduced modelling, as shown in the following section.

3 NON-DIMENSIONAL FORMULATION OF SHEET BENDING

Figure 6 shows the bending of a cantilever beam, i.e. a projection of the plate in Fig 1. The flexible transversal displacement is denoted as w. For the sake of deriving a proper similarity formulation, we perform model reduction and use the geometrically linearized (small strain and displacement) elasto-plastic theory of beams.

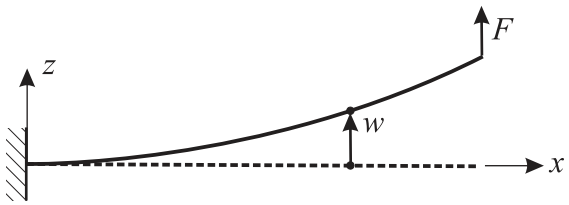

Figure 6: Bending of a beam/plate

In the framework of a quasi-static modeling, the bending moment follows to

$$M = -F(L-x). \tag{3}$$

3.1 Plastic zones

The bending moment as a resultant of the stress is written as

$$M = B\int \sigma(z) z dz. \tag{4}$$

In the elastic range, the distribution of the stress is linear over the cross-section. The yield moment corresponds to the state where the yield stress is reached at $z=H/2$, i.e. $M_Y = \frac{1}{6}\sigma_Y BH^2$. In the quasi-static case, the yield load follows from Eq. (3) by substituting $x=0$,

$$F_Y = \frac{BH^2\sigma_Y}{6L}. \tag{5}$$

If the load is higher than the yield load, the domain is divided into elastic and plastic zones as shown in Figure 7.

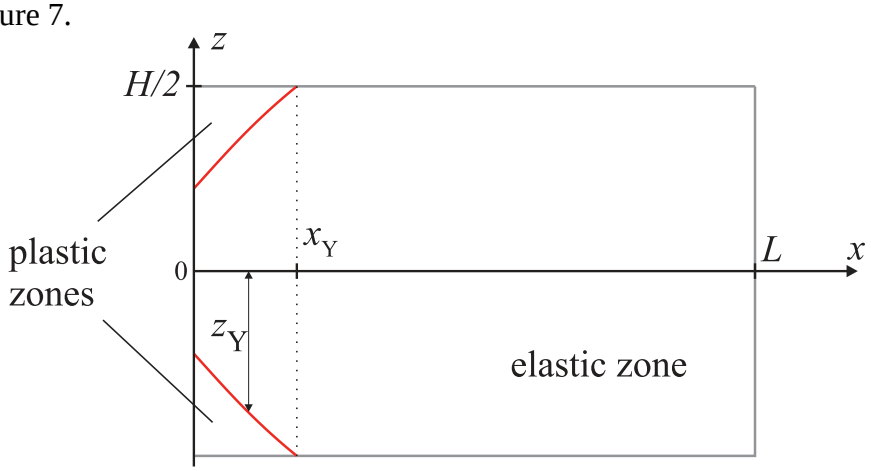

Figure 7: Elastic and plastic zones

Assuming that the deformations remain small and that the Bernoulli-Euler hypothesis for beams does hold, the axial strain is expressed as

$$\varepsilon = -zw''. \tag{6}$$

A prime denotes differentiation with respect to x. Thus, the stress in the elastic and plastic zones can be expressed by

$$\sigma = \sigma_Y \frac{z}{z_Y} \qquad \text{for } z \le z_Y, \tag{7}$$

$$\sigma = a\left(\frac{\sigma_Y}{E}\frac{z}{z_Y}\right)^b \qquad \text{for } z \ge z_Y.$$

The boundary z_Y of the plastic zone follows from equating Eqs. (3) and (4), using Eq. (7):

$$2B\left(\int_0^{z_Y} \sigma_Y \frac{z}{z_Y} z\,dz + \int_{z_Y}^{H/2} a\left(\frac{\sigma_Y}{E}\frac{z}{z_Y}\right)^b z\,dz\right) = -F(L-x). \tag{8}$$

Integration yields

$$\frac{\sigma_Y z_Y^2}{3} + a\left(\frac{\sigma_Y}{E z_Y}\right)^b \left(\frac{H^{b+2}}{2^b(4b+8)} - \frac{z_Y^{b+2}}{b+2}\right) = -\frac{F}{2B}(L-x). \tag{9}$$

From Eq. (9) the length x_Y of the plastic zone is obtained by substituting z_Y=H/2. An analytical solution is possible. The height z_Y of the plastic zone is obtained as a function of x. Due to the nonlinearity of the equation, z_Y has to be solved numerically.

3.2 Curvature

From Eqs. (1) and (6) follows that

$$\sigma_Y = -E z_Y w''. \tag{10}$$

Inserting Eq. (10) into Eq. (9) yields an equation for the curvature in the elasto-plastic case:

$$-\frac{w'' E z_Y^3}{3} + a\left(-w''\right)^b \left(\frac{H^{b+2}}{2^b(4b+8)} - \frac{z_Y^{b+2}}{b+2}\right) = -\frac{F}{2B}(L-x) \tag{11}$$

Due to the nonlinearity with respect to w'', only a numerical solution is possible. For the elastic range, $x > x_Y$, Eq. (11) simplifies to the well-known form

$$w'' = \frac{12F}{BH^3E}(L-x). \tag{12}$$

3.3 Normalization

In order to obtain a generalized representation, a normalization of the above equations has been performed as follows: By introducing the non-dimensional quantities

$$\xi = \frac{x}{L}, \quad \zeta = \frac{z}{L}, \quad H^* = \frac{H}{L}, \quad a^* = \frac{a}{E}, \quad F^* = \frac{F}{aLB}, \quad \sigma^* = \frac{\sigma}{E}, \tag{13}$$

Eq. (8) can be rewritten as

$$2a^{**}\zeta_Y^2(2+b-3(a^{**})^b)+3\left(\frac{1}{2}\right)^{1+b}a^*H^{*2}(a^{**}H^*\zeta_Y^{-1})^b=\frac{3}{2}F^*a^*(\xi-1)(2+b) \tag{14}$$

with

$$a^{**}=\left(a^*\right)^{\frac{1}{1-b}}. \tag{15}$$

Substituting $\zeta_Y = H^*/2$ and solving Eq. (14) yields the normalized extension ξ_Y of the plastic zone. On the other hand side, ζ_Y is obtained as a function of ξ. The normalized curvature and deflection are defined by

$$w^*=\frac{w}{L},\quad (w^*)''=Lw'' \tag{16}$$

and the following convention is used:

$$(w^*)''=\frac{d^2w^*}{d\xi^2}. \tag{17}$$

Substituting Eq. (13) into Eq. (11) yields the equation for the normalized curvature for the elasto-plastic range ($\xi \le \xi_Y$):

$$4(w^*)''\zeta_Y^3\left(2+b\right)+3a^*\left(-(w^*)''\right)^b\left(4\zeta_Y^2\left(\zeta_Y\right)^b-H^{*2}\left(H^*\right)^b\right)=3F^*a^*(2+b)\left(1-\xi\right) \tag{18}$$

Solving Eq. (18) numerically we obtain the curvature as a function of ξ. By numerical integration of Eq. (18) the deflection can be computed. Figure 8a shows the plastic tip displacement $w_{tip,plast}(L)$ as a function of the load F related to the yield force F_Y. In this dimensional representation, a separate curve is obtained for each configuration of H and L. However, in the non-dimensional representation in Figure 8b, in which non-dimensional quantities according to Eq. (13) are used, only one curve is obtained for the three cases.

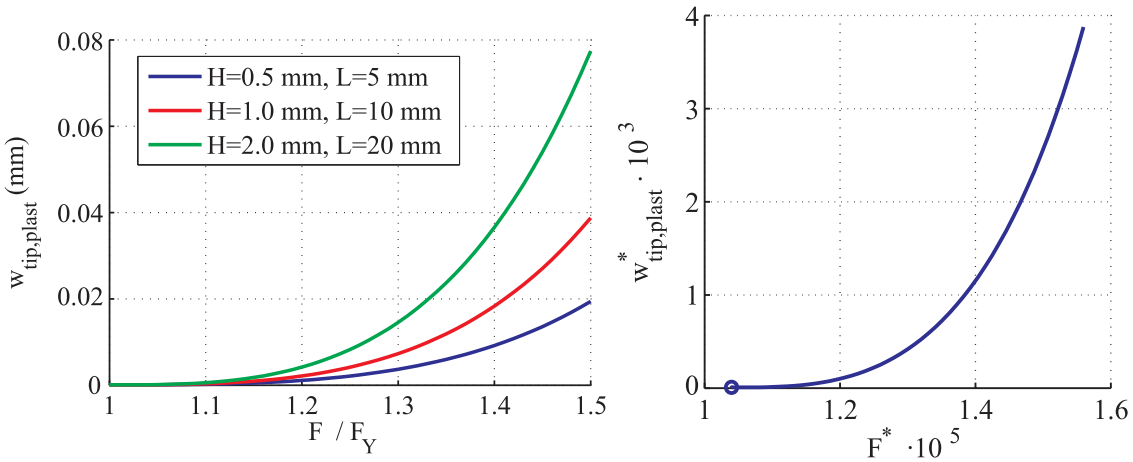

Figure 8: Plastic tip displacement (a) dimensional and (b) non-dimensional representation

3.4 Discussion of the non-dimensional formulation

In the dimensional representation with the coordinates x, the bending process is specified by eight physical quantities:

$$w, F, E, a, b, H, L, B. \tag{19}$$

On the other hand, in the dimensionless formulation derived in section 3.3 with the normalized coordinate $\xi = x / \mathrm{L}$ the number of essential parameters has been reduced to the following five non-dimensional quantities

$$\frac{w}{L}, \frac{F}{aBL}, \frac{a}{E}, b, \frac{H}{L}. \tag{20}$$

The results show that for the simple model of an elasto-plastic beam bending process the same normalized quantities have been derived as have been obtained by Baker et al. [1] using the Buckingham Pi theorem. For the large-deformation elasto-plastic bending problem with distributed loading, see also [3].

Recall that all the results in this section are based on the geometrically linear Bernoulli-Euler beam theory with exponential stress-strain relation. Thus the results are valid for small deformations. It has been shown in [3] that the non-dimensional parameters according to Eq. (20) are also suitable for a non-dimensional formulation in case of large strains. This gives evidence for using it by analogy also for the complex industrial sheet metal bending process.

3.5 Industrial application

The results of sections 3.1-3.4 have been applied to an industrial bending process. On a Salvagnini automatic panel bender, the bending forces for six bending processes (90° bending angle) have been measured for three sheet thicknesses (H_1, H_2, H_3) with two values for length (L_1, L_2) respectively. By measuring the forces of the drives, the resulting bending force has been computed. In Figure 9 the measured force for the six cases is shown as a function of the bending angle. In this representation the force is related to the maximum admissible force on the machine.

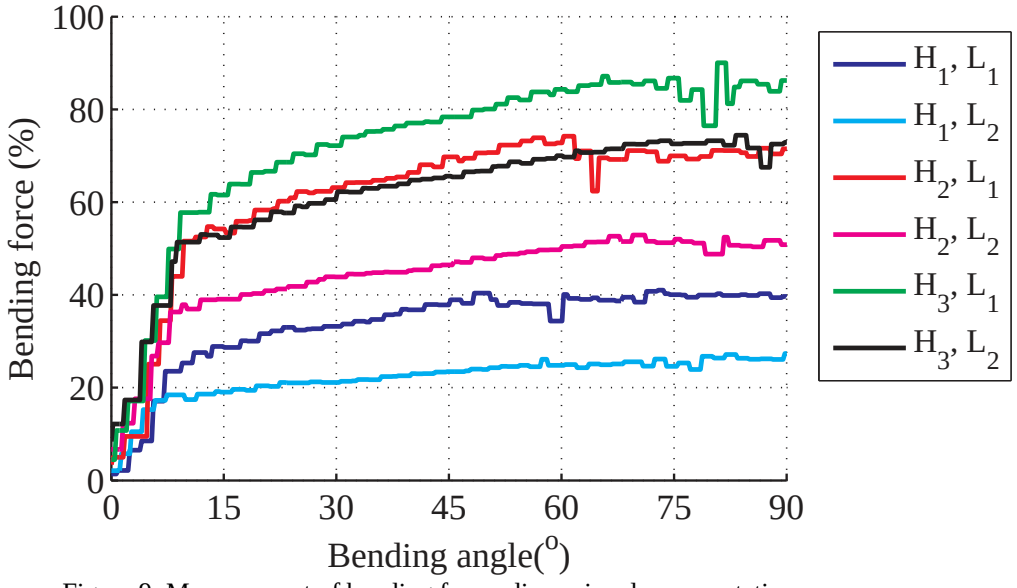

Figure 9: Measurement of bending force, dimensional representation

The normalized bending force according to Eq. (20) is shown in Figure 10. The normalized representation demonstrates the reduction of complexity by utilizing similarity of several parameter combinations. The concept of similarity is a powerful tool for analyzing complex physical processes.

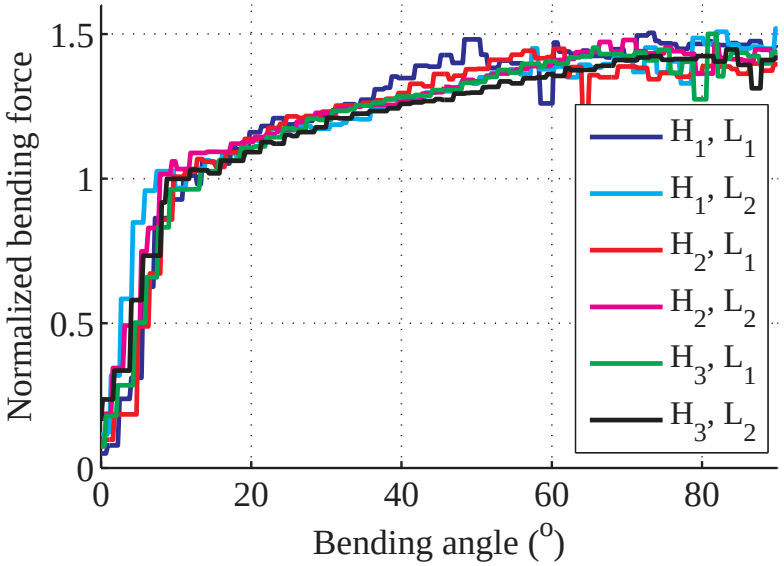

Figure 10: Measurement of bending force, normalized representation

4 CONCLUSIONS

For an industrial bending process two strategies for reducing the numerical effort of parameter studies have been investigated. First, an efficient and precise Finite Element formulation based on continuum shell elements has been investigated. Secondly it has been shown how it is possible to find similar configurations by an appropriate non-dimensional formulation. The method has been verified by measurements on an industrial bending machine. These two strategies are very powerful tools for optimizing the bending process.

ACKNOWLEDGMENT

This work has been supported by the Austrian COMETK2 program of the Linz Center of Mechatronics (LCM), and was funded by the Austrian federal government and the federal state of Upper Austria.

REFERENCES

[1] W.E. Baker, P.S. Westine, F.T. Dodge, *Similarity Methods in Engineering Dynamics, Theory and Practice of Scale Modeling*, Elsevier, 1991.

[2] L.I. Sedov, *Similarity and Dimensional Methods in Mechanics*, CRC Press, 1993.

[3] Ch. Zehetner, F. Hammelmüller, H. Irschik, W. Kunze, Similarity Methods in Elasto-Plastic Beam Bending. E. Oñate, D.R.J. Owen, D. Peric and M. Chiumenti eds. *XIII International Conference on Computational Plasticity (COMPLAS XIII)*. Barcelona, Spain, September 1-3, 2015.

[4] W.F. Chen, D.J. Han, *Plasticity for Structural Engineers*, J.Ross Publishing (2007)

[5] Abaqus 6.14 Documentation, Dassault Systèmes, 2015